

## HYDRATED PROPERTIES OF COMPOSITE SYSTEMS FOR WATER AND SOIL REMEDIATION ON THE BASIS OF NANOSILICAS AND YEAST CELLS

Tetyana Krupskaya<sup>1</sup>, Natalya Klymenko<sup>1</sup>, Alina Holovan<sup>1, ✉</sup>,  
Alyona Novikova<sup>1</sup>, Volodymyr Turov<sup>1</sup>

<https://doi.org/10.23939/chcht16.04.630>

**Abstract.** The method of low-temperature <sup>1</sup>H NMR spectroscopy is applied to study the hydrated properties of bio-nanocomposite created on the basis of the mixture of hydrophobic and hydrophilic silicas (AM1-300 and A-300 with ratio of 1:1), water, *n*-decane, and yeast cells. The produced mixture of nanosilicas contributes to mitosis and cell growth. It is shown that the cause of activation of their vital processes may be related to the formation of the system of water polyassociates, which change the conditions of substance transport through the cell membranes, on the phase boundaries of solid particles and aqueous medium.

**Keywords:** <sup>1</sup>H NMR spectroscopy, strongly and weakly associated water, remediation, bakery yeast.

### 1. Introduction

The problem of purification of contaminated with oil products water and soil becomes more and more urgent year by year.<sup>1-5</sup> There are three main methods of water purification: mechanical, physico-chemical, and biological. However, the first two methods do not solve the problem of pollution utilization, and in some cases, for example when using surfactants, may do more damage to the nature than oil pollution. That is why the method of water and soil bioremediation, based on the oxidation of oil products by microorganisms, is at present the most promising.<sup>6-10</sup>

Microorganisms which use hydrocarbons are widely spread in the nature. The active forms of microorganisms are isolated from the different aquatic and soil ecosystems, especially from the contaminated with

hydrocarbons and oil ones and from the microbial flora of oil and oil-field waters.<sup>11-13</sup> 22 bacteria genera, 31 micro-mycetes genera, as well as 19 yeast genera, isolated from the soil ecosystems, are described, which are capable of biodegradation of different oil hydrocarbons.<sup>12,14-18</sup> Choice of the active microorganism-destroyer of hydrocarbon pollution should be made with account for a set of requirements. One must consider that introduced into soil biomass should not be alien to the soil microflora. Another important requirement to the introduced into soil microorganisms is their non-pathogenicity. The microbial cells may be affected by adverse environmental conditions, hence the microorganism-destroyer should possess high vital capacity.<sup>19</sup>

By now, many types of bacterial preparations qualified for common use has been developed: a series of biopreparations «Naftoks» with a bacterial culture on the basis of the strain *Pseudomonas citroneolis* allows to purify contaminated with oils soil. The cleaning time is from 3 to 6 months. The aerobic oil-oxidizing bacteria, such as the *Micobacterium phlei*, *Pseudomonas aeruginosa*, and *Rhodococcus species* have the same properties and activity. The preparations Noggies NG20 by the brand Biodetox, Para-Bac, (by the brand Micro-Bac, USA) and many others.<sup>20</sup>

As long as all commercially available biopreparations have living bacterial strains, their efficiency depends heavily on the environmental conditions, storage life, and presence of related substances ensuring the nutrition and bacterial growth in soil and water. The studies, undertaken in the Ukrainian scientific centers,<sup>21,22</sup> approve that nanodisperse particles may have stimulating influence on microorganisms, which depends largely on the formation of water layers with partially destroyed hydrogen-bond network at the boundary between cell and particle.<sup>23</sup> Such weakly associated water is capable of dissolving the complex organic molecules, appearing in vital cellular processes, which accelerates their metabolism. It was also demonstrated that yeast cells and some other microorganisms significantly accelerated the fission process in

<sup>1</sup> Chuiko Institute of Surface Chemistry of the National Academy of Sciences of Ukraine

17, General Naumov St., Kyiv 03164, Ukraine

✉ [a.golovan2020@gmail.com](mailto:a.golovan2020@gmail.com)

© Krupskaya T., Klymenko N., Holovan A., Novikova A., Turov V., 2022

the presence of nanodisperse silicas.<sup>22</sup> Moreover, nanodisperse materials due to their high adsorptive capacity in relation to different types of organic and inorganic compounds may act as carriers of nutritional substances, providing the long-term functioning of bacterial cultures. Thus, the perspective direction of improvement of performance characteristics of hydrocarbon biodecomposers may be an integration of the nanobiocomposite system created on the basis of cell cultures, mixture of nanosilicas with certain hydrophobic and hydrophilic properties and related substances, providing the contact of composite components with hydrocarbon and aqueous mediums and enabling the adjustment of cell cultures to environmental conditions.

Thus, the objective of the present study is to investigate the applicability of model system consisting of yeast cells and taken in equal quantity hydrophobic (AM1-300) and hydrophilic (A-300) silicas for oxidation of hydrocarbons. The vital capacity of yeast cells after their contact with nanosilicas under the conditions of low and high hydration of composite system, as well as the water condition in the nanocomposite consisting of fixed amount of water and hydrocarbon (*n*-decane) has also been investigated.

This raises the problem of wetting water with hydrophobic powder materials, which was solved by using the process of moistening the powders with water using dosed mechanical loads.<sup>24</sup>

Hydrophobic particles interact with the aqueous medium by means of van der Waals forces, and the state of the colloidal system strongly depends on the concentration of the dispersion medium.<sup>25</sup> Since a complex heterogeneous system tends to minimize free energy, depending on the amount of water, the formation of stable colloids or colloids containing adsorbed air microbubbles (which rise to the upper part of the vessel) is possible.

## 2. Materials and Methods

### 2.1. Materials

At the Chuiko Institute of Surface Chemistry of the NAS of Ukraine methods for producing composite systems based on hydrophilic A-300 and hydrophobic AM-1-300 silicas, as well as polymethylsiloxane were developed. As a result of studies based on equal amounts of hydrophobic or porous polymethylsiloxane and hydrophilic nanosilica A-300, it was shown that when the composite system is formed, the specific surface of the material decreases significantly, which is associated with close contact between hydrophobic and hydrophilic particles. When water is added to the composite system, during homogenization under conditions of dosed mecha-

nical load, the effect of nanocoagulation is manifested.<sup>25,26</sup> The dry bakery yeast culture *Saccharomyces cerevisiae* has been used. In the process of sample preparation, the cell mass was carefully ground without major mechanical loading with the portion of mixture 1:1 of methyl silica AM1-300 and silica A-300, produced on the Kalush Pilot Plant of the Chuiko Institute of Surface Chemistry. Then distilled water and mass of *n*-decane in the quantity of 40 and 15 wt % of dry mass of yeast cells was added to the mixture. The mixture was extensively stirred until a homogeneous mass was obtained. Such composite system may be easily introduced into the aqueous medium while wetting its hydrophobic and hydrophilic components. The NMR measurements were taken in standard 5 mm ampules.

### 2.2. Microscopy

Microphotography of powders and emulsions was performed with the use of a microscope Primo Star (Zeiss, Germany) with  $\times 100$  and  $\times 1000$  magnification with immersion.

TEM images were obtained on a JEOL JEM 2010F microscope at the accelerating voltage of 160kV. The samples were dissolved in deionized water via sonication and dried on a cooper grid.

### 2.3. $^1\text{H}$ NMR Spectroscopy

The NMR spectra were recorded using an NMR spectrometer of high-resolution Varian Mercury (operating frequency 400 MHz). Eight  $60^\circ$  probe pulses with a duration of 1  $\mu\text{s}$  and bandwidth of 20 kHz were used. The temperature was controlled by Bruker VT-1000 device with relative mean errors  $\pm 1$  K. The intensity of signals was determined by measurement of area of peaks by applying the procedure of signal decomposition in assumption of the Gaussian signal shape and optimization of zero line and phase with relative mean errors not lower than 5 % for well resolved signals and  $\pm 10$  % for interlocking signals. To prevent supercooling of water in the studied objects, the measurements of the concentration of unfrozen water were carried out on heating of samples preliminarily cooled to 210 K. The temperature dependencies of NMR signals intensity were carried out in automated cycle where the sample storage time at a constant temperature was 9 min, and measuring time was 1 min.<sup>23,27</sup>

The main parameter, determining the structure of hydrogen-bond network, was the value of proton chemical shift ( $\delta_H$ ). It was expected that water, each molecule of which takes part in the formation of four hydrogen bonds (two by protons and two by electron lone pairs of oxygen atoms), has the chemical shift  $\delta_H = 7$  ppm (for hexagonal ice), and weakly associated water (which does not take

part in the formation of hydrogen bonds as a proton donor) has the chemical shift  $\delta_H = 1-1.5$  ppm.<sup>23,27</sup> In order to determine the geometrical dimension of clusters of adsorbed water, the Gibbs-Thomson relation was used, associating the radius of spherical or cylindrical water cluster or domain ( $R$ ) with the freezing point depression:<sup>28-30</sup>

$$\Delta T_m = T_m(R) - T_{m,\infty} = \frac{2\sigma_{sl}T_{m,\infty}}{\Delta H_f \rho R}, \quad (1)$$

where  $T_m(R)$  is the melting point of ice, localized in the pores of radius  $R$ ,  $T_{m,\infty}$  is the melting point of volumetric ice,  $\rho$  is the density matrix,  $\sigma_{sl}$  is the interaction energy between solid object and liquid, and  $\Delta H_f$  is volumetric melting enthalpy. For practical use, Eq. (1) may be applied as  $\Delta T_m = (k/R)$ , in which the constant  $k$  for many heterogeneous systems containing water is close to 50 grad·nm.<sup>27</sup> The procedure of taking NMR-measurements and methods of measuring radii of clusters of interfacial water are described in detail in the works.<sup>23,27</sup> In this case, it is fair to say that the polyassociates with  $R < 2$  nm are clusters, and polyassociates of the bigger size are domains or nanodrops, as they contain several thousands of water molecules.<sup>27</sup>

The process of freezing (fluctuation) of bound water corresponds to the changes in the Gibbs free energy, conditioned upon the effects of limited space and nature of interfacial surface. Difference from the process in volume is the less, the further from the surface the water layer is. The water, characteristics of which correspond to the volumetric water, freezes at 273 K, and when the temperature decreases (excluding the effect of overcooling), the layers of water, which are close to the surface, freeze. For the change in free energy of bound water (ice), the following proportion holds true:

$$\Delta G_{ice} = -0.036(273.15 - T), \quad (2)$$

where the numeral coefficient is a parameter, related to the temperature coefficient of the change in the Gibbs free energy for ice.<sup>28</sup> By determining the temperature dependence of nonfreezing water concentration  $C_{uw}(T)$  from the intensity value of signal, one may calculate the amount of strongly and weakly associated water and thermodynamic characteristics of these layers.<sup>23,27</sup>

Interfacial energy of water on the boundary with solid particles or in its aqueous solutions was determined as the module of total decrease of water free energy, conditional upon the presence of the phase boundary<sup>23,27</sup> by formula:

$$\gamma_s = -K \int_0^{C_{uw}^{\max}} \Delta G(C_{uw}) dC_{uw}, \quad (3)$$

where  $C_{uw}^{\max}$  is the total amount of nonfreezing water at a temperature of 273 K.

### 3. Results and Discussion

Fig. 1 shows TEM microphotographs of a composite system consisting of a mixture of hydrophilic A-300 and hydrophobic AM-1-300 silicas whereas in Fig. 2, optical photographs of the composite system consisting of *S. cerevisiae* yeast cells, mixture of nanosilicas, water, and *n*-decane are given. Biocomposite is a mixture of conglomerates of yeast cells and particles of nanosilicas mixture (Fig. 2a). In the composite system, there are cells of different sizes, forming in the process of their fission; one may observe a fair amount of newly formed daughter cells (Fig. 2b). Therefore, used under the composite production, mixture of nanosilicas enables their fission even in the absence of natural for the chosen type of yeast cells nutritional medium (simple sugars). One may assume that, in the absence of carbohydrates, the nutrition of yeast cells may be provided by hydrocarbons.

When a small amount of water is added to the composite, the latter easily forms a film without visible signs of layer separation (Fig. 2c), in which yeast cells assume almost spherical shape, and silica particles appear as agglomerates with the size of 10  $\mu\text{m}$  and more.

The influence of a nanocomposite system on the vital activity of *S. cerevisiae* cells suspension was investigated in the presence of 10 % sucrose solution (without any microelements). The kinetic curves of  $\text{CO}_2$  evolution by cell suspension in the presence of composite of different concentrations, including the mixture of silicas, yeasts, water, and *n*-decane are given in Fig. 3. Four samples consisting of weighed amounts of bionanocomposite (mixture 1:1 of nanosilicas and yeast cells) weighing 0.2 g (sample 1) and 1 g (sample 3) were analyzed. Weighed amounts of the pure culture *S. cerevisiae* (0.1 g – sample 2 and 0.5 g – sample 4) were used as control (Fig. 3a). The diagram of evolution of average amount of  $\text{CO}_2$  by the suspension of bakery yeasts cells in 15 days is given in Fig. 2b.

As it may be seen from Fig. 3a, in the initial stage of fermentation process, the dynamic evolution of  $\text{CO}_2$  occurs, which is connected with the presence of sufficient amount of nutritional substances in a solution. Then the gas evolution slows due to the formation of by-products of yeasts (ethanol and  $\text{CO}_2$ ) and decrease of the amount of sucrose (Fig. 3a). However, in the following the metabolism of yeast cells changes, and they start to process carbohydrates which appear in the form of *n*-decane in the samples 1 and 3. This implies that the process of gas evolution may continue even if the resources of sucrose in a system have been depleted.

The attained results demonstrate noticeably intenser gas evolution in the samples 1 and 3 in comparison with the control (samples 2 and 4) (ref. to the diagram given in Fig. 3b). Hence the mixture of nanosilicas has a

significant activating influence on the processes of vital activity of *S. cerevisiae* cells in the selected range of solid phase concentrations. This confirms a hypothesis about

the feasibility of creating effective bionanocomposites for remediation of contaminated with hydrocarbons water and soil.

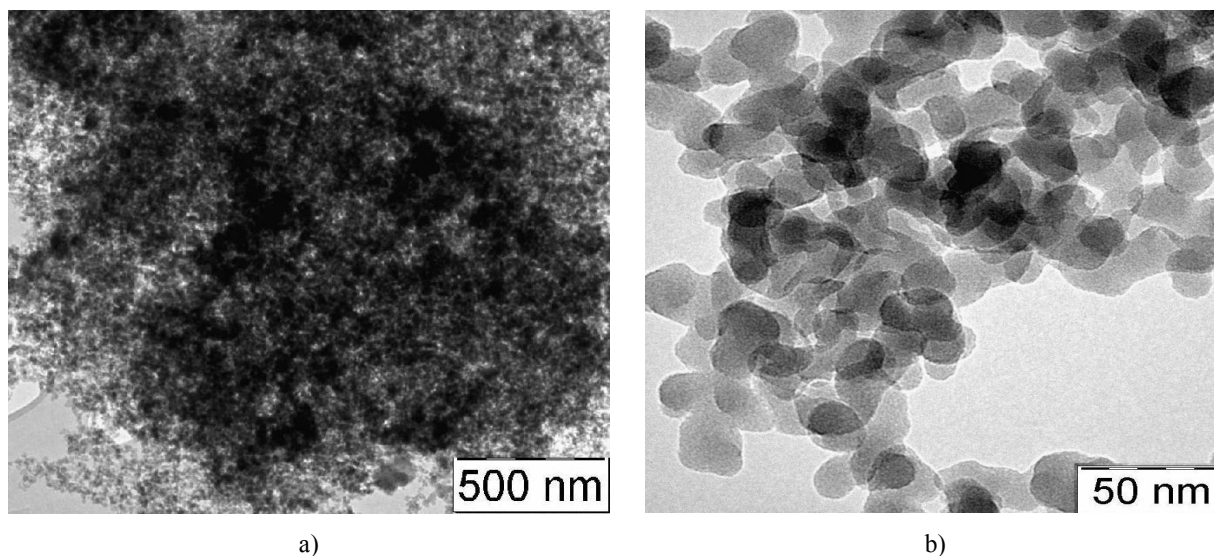


**Fig. 1.** TEM images of selected samples of composites A-300 + AM1, at different magnifications

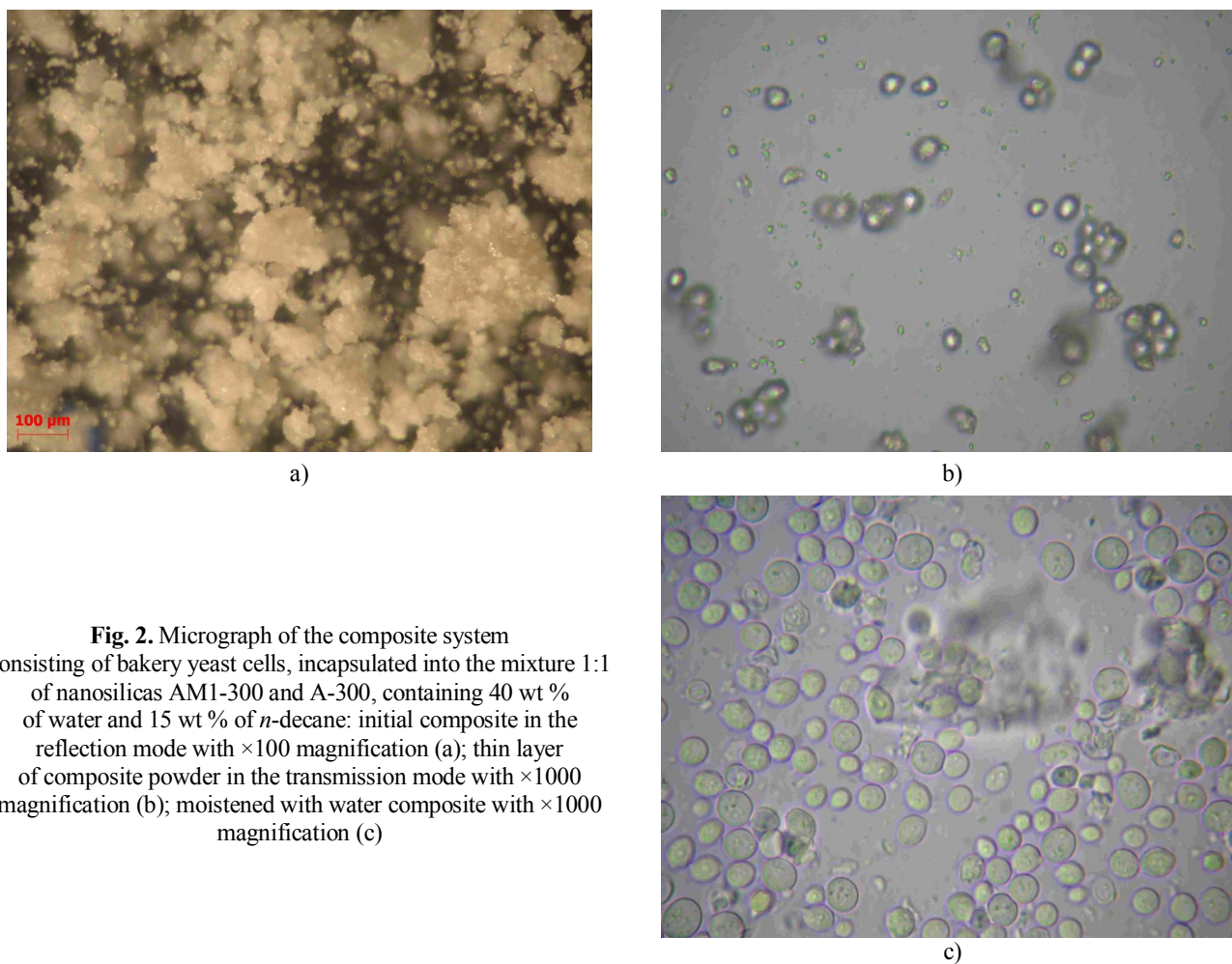


**Fig. 2.** Micrograph of the composite system consisting of bakery yeast cells, encapsulated into the mixture 1:1 of nanosilicas AM1-300 and A-300, containing 40 wt % of water and 15 wt % of *n*-decane: initial composite in the reflection mode with  $\times 100$  magnification (a); thin layer of composite powder in the transmission mode with  $\times 1000$  magnification (b); moistened with water composite with  $\times 1000$  magnification (c)

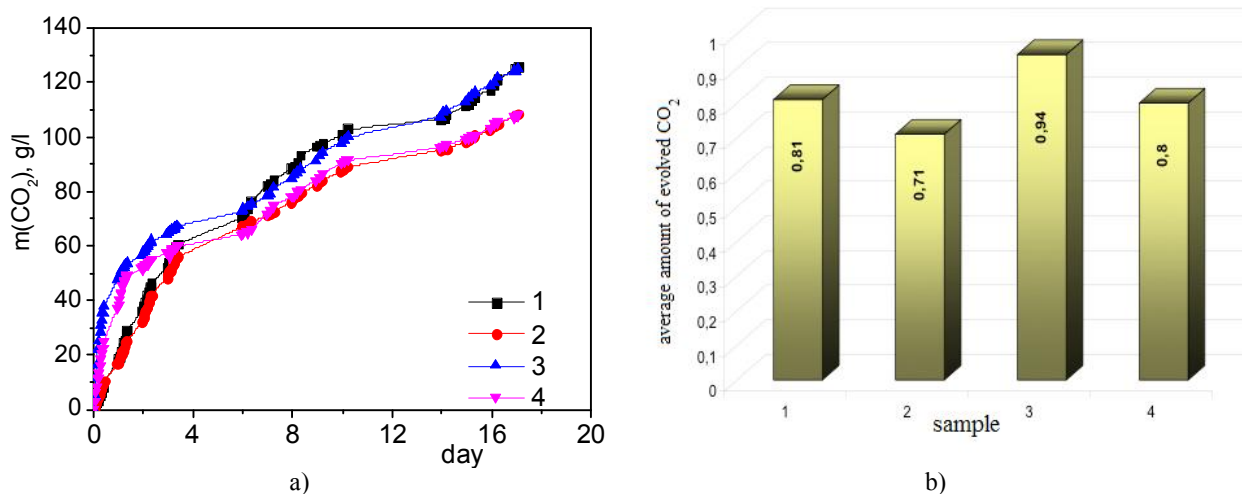


**Fig. 3.** The kinetic curves of CO<sub>2</sub> evolution by suspension of bakery yeast cells in the presence of the composite system in the samples of composite weighing 0.2 g (1) and 1 g (3) in comparison with the pure culture *S. cerevisiae* 0.1 g (2) and 0.5 g (4) (a), the diagram of evolution of average amount of CO<sub>2</sub> by the suspension of bakery yeasts cells in 15 days (b)

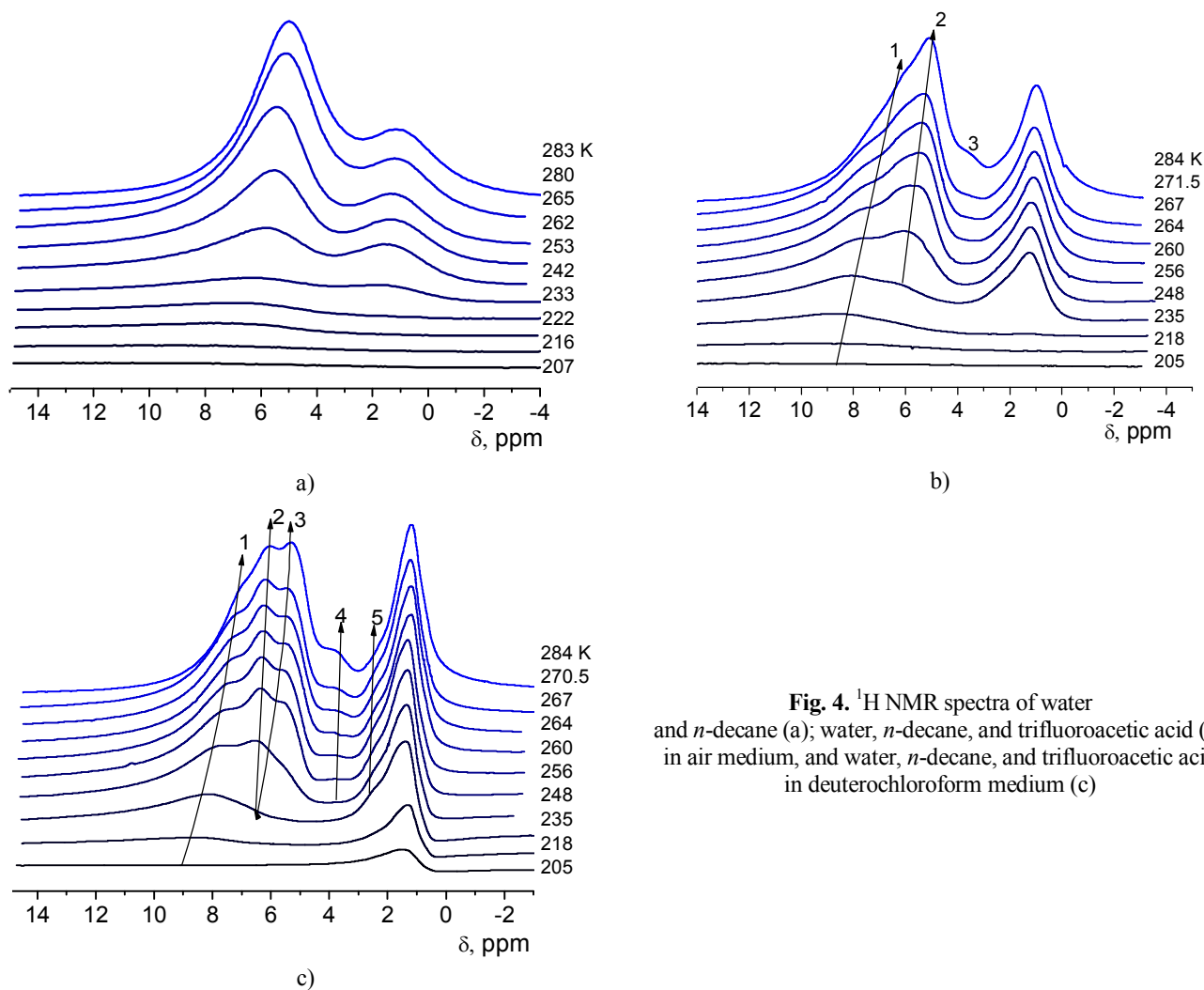


**Fig. 4.** <sup>1</sup>H NMR spectra of water and *n*-decane (a); water, *n*-decane, and trifluoroacetic acid (b) in air medium, and water, *n*-decane, and trifluoroacetic acid in deuteriochloroform medium (c)

The cause of activating influence of the mixture of hydrophobic and hydrophilic silicas on the vital processes of yeast cells may consist in the formation of surface-bound clusters or water domains, the characteristics of which differ significantly from the volumetric, on the phase boundaries of composite and aqueous medium. In these circumstances the activation of cell receptors in glycocalyx of yeast cells may occur and the conditions of mass transport of nutritional substances and products of cell metabolism through the cell membrane may change.

$^1\text{H}$  NMR spectra of composite consisting of yeast cells, water, and *n*-decane are given in Fig. 4a. In the spectra, signals of water (intenser signal) and *n*-decane were recorded. Since the amount of water is only 40 wt % of dry yeast mass, the major part of it probably composes the intracellular liquid. With the reduction of temperature the intensities of water and *n*-decane signals decrease due to their partial freezing. With the reduction of temperature, the chemical shift of water protons increases from  $\delta_H = 4.8$  ppm at  $T = 283$  K to  $\delta_H = 7$  ppm at  $T = 207$  K. This is due to the increase of orderliness of water polyassociates, which are constituents of intracellular structures.<sup>27</sup> In accordance with the association degree of responsible for this signal water, one may refer it to the strongly associated water (SAW), in which the structure of hydrogen-bond network is a little more ordered than in liquid water.

In Fig. 5, the nonfreezing water concentration – temperature diagram is given, and in Fig. 5b there is a radial distribution of intracellular water clusters constructed on its basis according to Eq. (1). Since the part of water that freezes at  $T < 265$  K is strongly bound water (SBW),<sup>27</sup> one may assume that the amount of weakly bound water (WBW) is only 80 mg/g of intracellular water. On the radial distribution of bound water clusters only one maximum at  $R = 5$  nm was recorded. In accordance with the change in freezing temperature of interfacial water one may calculate the change in the Gibbs free energy ( $\Delta G(C_{uw})$ , Eq. (2)). Then the area, limited by the dependency diagram  $\Delta G(C_{uw})$ , will determine the interfacial energy, *i.e.*, the total decrease of water free energy conditional upon the presence of the phase boundary ( $\gamma_S = 14$  J/g), which may be calculated according to Eq. (3).<sup>23,27</sup>

One of the products, which may appear in water suspensions in the process of aerobic fermentation, is acetic acid. Penetrating the yeast cells, it holds down the process of alcoholic fermentation, and if its concentration is above 0.2 %, the vital activity of yeasts is completely suppressed.<sup>27</sup> However, the carboxylic acids may be used for differentiation of composition of different types of cluster structures, which are present in yeast cells.<sup>27</sup> Since the size of the proton chemical shift in acids is significantly larger than in water and is up to 11 ppm, the

intracellular water may be differentiated in accordance with its ability to dissolve acid.

Recorded at different temperatures spectra of the compatible signal of trifluoroacetic acid (TFA) and water, when adding TFA in the quantity of 30 % from the mass of dry yeasts to the composite, are given in Fig. 3b. When the acid is added, the water signal splits into two signals, each of which may have several constituents. The difference in the chemical shift sizes is determined by the concentration of TFA dissolved in polyassociates of bound by cells water.

The dependency of concentration of the non-freezing mixture  $\text{H}_2\text{O}$ -TFA on the temperature is given in Fig. 5c. Signal 1 corresponds to the polyassociates (clusters or domains) of SAW, consisting of more concentrated TFA solution. From such solutions water crystallizes at lower temperatures. As the temperature decreases, the chemical shift of the signals 1 and 2 increases, which is conditional upon the increase of TFA concentration in nonfreezing water during the process of ice crystals formation. The minimum value of the chemical shift of solution responsible for the signal 2 is  $\delta_H = 4.8$  ppm, which corresponds to the chemical shift of pure water (Fig. 3a). At  $T = 283$  K in spectra appears the signal 3 with the chemical shift  $\delta_H = 3.8$  ppm, which corresponds to the water polyassociates with partially destroyed hydrogen-bond network.

If one assumes that during the freezing process water and TFA do not form mixed crystals and freeze in the form of individual substances, during the heating of pre-cooled samples the nanocrystals of frozen acid and water melt, and only then their solution forms, which is recorded in the form of a merged NMR signal of acid and water. In this case, one may use the Gibbs-Thomson relation in order to estimate the sizes of ice crystallites (Eq. (1), Fig. 5d).

On the distributions  $\Delta C(R)$ , two maxima in the range  $R < 10$  nm are observed. For the signal 1, these maxima are shifted to the range of the less values of  $R$ . Comparing the distribution, obtained for the polyassociates responsible for the signal 2, to the given in Fig. 3b distributions (without TFA), one may conclude that acidification of the system makes the distribution narrower, and also on it there is a raised area, which corresponds to the formation of domains with  $R = 30$  nm. It means that even if the responsible for the signal 2 polyassociates practically do not contain any TFA, its presence in cells causes the significant change of the structure of intracellular water clusters.

The sample, spectral characteristics of which are given in Figs. 4b and 5c, d, is a complex of closely spaced composite particles, gaps between which are filled with air. Such phase heterogeneity determines fairly large line width in NMR spectra. In Figs. 4c and 5e, f, the recorded

at different temperatures  $^1\text{H}$  NMR spectra (Fig. 4c) and calculated on their basis dependencies of change in the concentration of nonfreezing mixture  $\text{H}_2\text{O}$ -TFA (Fig. 5e)

are given, as well as the radial distributions of fluctuating water nanocrystals corresponding to the different lines in spectra (Fig. 5f).

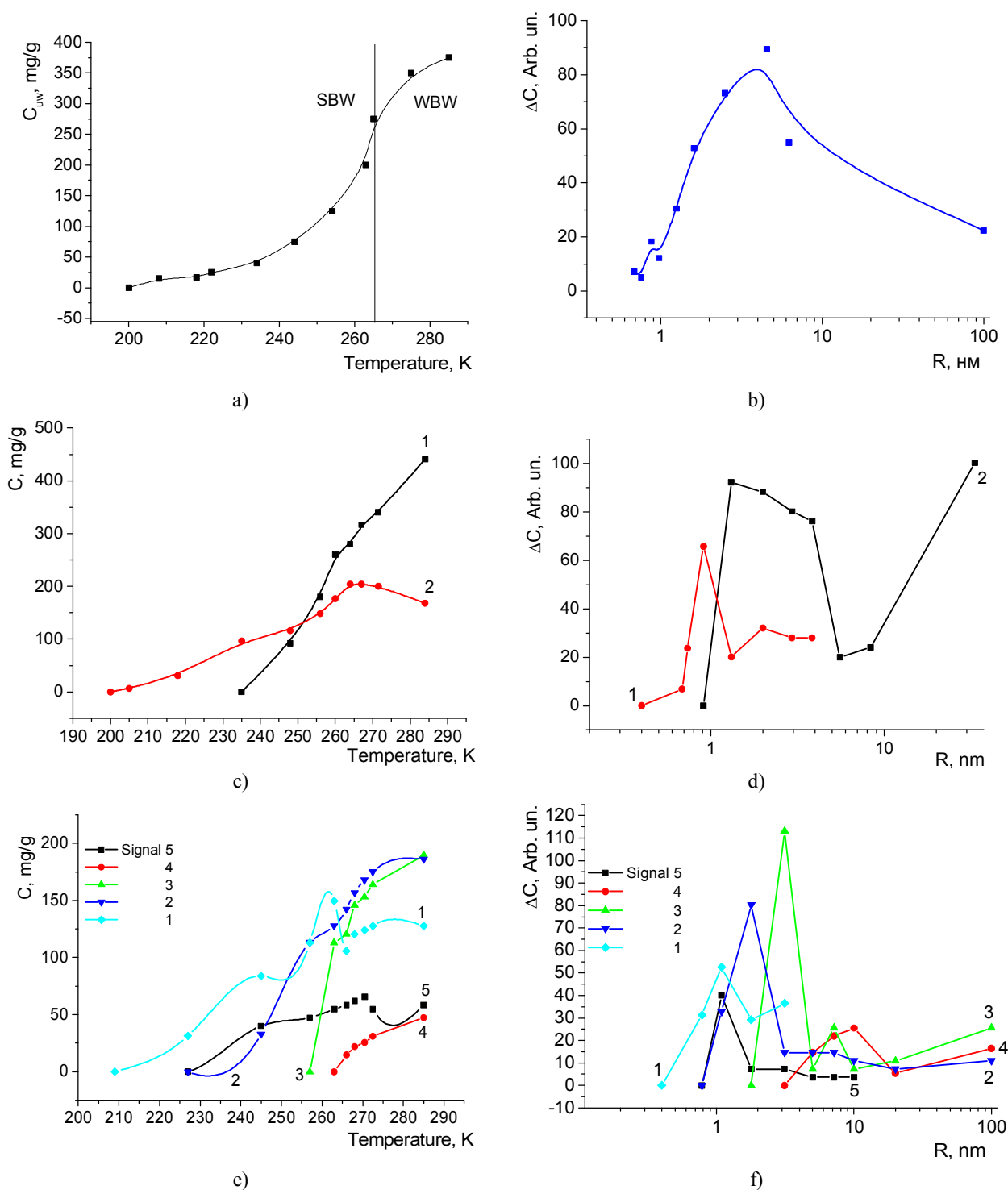


**Fig. 5.** Temperature dependencies of nonfreezing water (a, c, e) and radial distributions of bound water clusters (b, d, f) in the composite system A-300:AM1-300 in the presence of  $n$ -decane (a, b),  $n$ -decane and TFA (c, d),  $n$ -decane, TFA, and chloroform (e, f)

The less line width in spectra allows to detect the fine structure of the signal. As it may be seen from the Fig. 4c, the signal 2 (Fig. 4b) is divided into two signals (2, 3, Fig. 4c). In this case, the signal 2 (Fig. 4c) is conditional upon the polyassociates of SAW capable of dissolving a small amount of TFA. The signal 4 (the analogue of the signal 3 in Fig. 4b) is conditional upon the water with partially destroyed hydrogen-bond network and appears in wide temperature range, which allows to determine the radial distribution of non-freezing water clusters for it (Fig. 5f). On the left side of the signal of methylene groups of *n*-decane there is a low-intensity signal, which may be referred to the weakly associated water (WAW), the molecules of which do not form hydrogen bonds. Such water may exist on the phase boundary of composite in the form of concentrated solution with hydrophobic components (*n*-decane, CDCl<sub>3</sub>).<sup>27</sup>

From the given in Fig. 5f radial distributions of fluctuating water clusters, it follows that water, which forms concentrated solutions of TFA (the signal 1), crystallizes in the form of nanocrystals, a major part of which has  $R = 1$  nm. The maxima of distributions for water, responsible for the signals 2 and 3, correspond to the radii  $R = 2$  and 3 nm, respectively. The water with partially destroyed hydrogen-bond network (the signal 4) composes polyassociates with  $R = 10$  nm and more. Weakly associated water (the signal 5) crystallizes in the form of crystallites with  $R = 1$  nm.

## 4. Conclusions

On the basis of mixture of hydrophobic and hydrophilic silicas (AM1-300 and A-300, respectively), water, *n*-decane, and yeast cells, a bionanocomposite system may be created, which allows to destruct hydrocarbons in aqueous medium. It is demonstrated that the chosen mixture of silicas activates the processes of cell fission not only in aqueous medium, but also in the composite itself.

The cause of activation of vital processes of yeast cells may be related to the formation of the system of water polyassociates, which change the conditions of substance transport through the cell membranes, on the phase boundaries of solid particles and aqueous medium. On the phase boundary a possibility of concurrent existence of several types of polyassociates of strongly associated water, which dissolve carboxylic acids (and probably other polar organic compounds) in different ways, and weakly associated water, which easily intermixes with nonpolar substances, such as many hydrocarbons was recorded. As a result, this may simplify the transfer of nutrients (sugars and hydrocarbons) into

cells and removal of metabolism products (CO<sub>2</sub>, ethanol, carboxylic acids) from cells.

## References

- [1] Chen, S.; Zhong, M. *Bioremediation of Petroleum-Contaminated Soil*. In *Environmental Chemistry and Recent Pollution Control Approaches*; Saldarriaga Noreña, H.A., Ed.; IntechOpen: London, 2019. <https://doi.org/10.5772/intechopen.90289>
- [2] Wang, X.; Zheng, J.; Han, Z.; Chen, H. Bioremediation of Crude Oil-Contaminated Soil by Hydrocarbon-Degrading Microorganisms Immobilized on Humic Acid-Modified Biofuel Ash. *J. Chem. Technol. Biotechnol.* **2019**, *94*(6), 1904–1912. <https://doi.org/10.1002/jctb.5969>
- [3] Malovanyy, M.; Petrushka, K.; Petrushka, I. Improvement of Adsorption-Ion-Exchange Processes for Waste and Mine Water Purification. *Chem. Chem. Technol.* **2019**, *13*(3), 372–376. <https://doi.org/10.23939/chcht13.03.372>
- [4] Afzal, M.; Rehman, K.; Shabir, G.; Tahseen, R.; Ijaz, A.; Hashmat, A.J.; Brix, H. Large-Scale Remediation of Oil-Contaminated Water Using Floating Treatment Wetlands. *NPJ Clean Water* **2019**, *2*, 3. <https://doi.org/10.1038/s41545-018-0025-7>
- [5] Kowalska, A.; Grobelak, A. Immobilisation of Selected Bacteria for Remediation on Various Media. *Inż. Ochr. Śr.* **2018**, *21*(4), 461–472. <https://doi.org/10.17512/ios.2018.4.11>
- [6] Cheng, J. Bioremediation of Contaminated Water-Based on Various Technologies. *Open Access Libr. PrePrints* [Online] **2014**, *3*, 1-13. <https://doi.org/10.4236/oalib.preprints.1200056> (accessed October 1, 2022).
- [7] Coelho, L.M.; Rezende, H.C.; Coelho, L.M.; de Sousa, P.A.R.; Melo, D.F.O.; Coelho, N.M.M. *Bioremediation of Polluted Waters Using Microorganisms*. In *Advances in Bioremediation of Wastewater and Polluted Soil*; Shiomi, N., Ed.; IntechOpen: London, 2015. <https://doi.org/10.5772/60770>
- [8] Shestopalov, O.V.; Bakharieva, G.Yu.; Mamedova, O.O.; Tverdokhliebova, N.Ye.; Yershov, D.I.; Mikheienko (Yashenko), L.O.; Sobol, Yu.O.; Yevtushenko, N.S.; Vas'kovets, L.A.; Chirkina, M.A. *Okhorona Navkolyshn'oho Seredovyshcha vid Zabrudnennya Naftoproduktamy: Navch. Posib.*; NTU "KhPI": Kharkiv, 2015.
- [9] Korchak, B.; Grynshyn, O.; Chervinskyy, T.; Nagursky, A.; Stadnik, V. Integrated Regeneration Method for Used Mineral Motor Oils. *Chem. Chem. Technol.* **2021**, *15*(2), 239–246. <https://doi.org/10.23939/chcht15.02.239>
- [10] Loginova, O.O.; Dang, T.T.; Belousova, E.V.; Shalimova, S.S.; Shevchenko, M.Yu.; Grabovich M.Yu. Boidegradatsiya Nefteproduktov v Pochve Shtammami Mikroorganizmov Roda *Acinetobacter*. *Organizatsiya i Regulyatsiya Fiziologo-Biokhimičeskikh Processov* **2010**, (12), 129–136.
- [11] Zhao, Z.; Wong, J.W.C. Biosurfactants from *Acinetobacter calcoaceticus* BU03 Enhance the Solubility and Biodegradation of Phenanthrene. *Environ. Technol.* **2009**, *30*(3), 291–299. <https://doi.org/10.1080/09593330802630801>
- [12] Toren, A.; Navon-Venezia, S.; Ron, E.Z.; Rosenberg, E. Emulsifying Activities of Purified Alaskan Proteins from *Acinetobacter radioresistens* KA53. *Appl. Environ. Microbiol.* **2001**, *67*(3), 1102–1106. <https://doi.org/10.1128/AEM.67.3.1102-1106.2001>
- [13] Khokhlov, A.; Strelko, V.; Khokhlova, L. Physico-Chemical Features of Bioactive Carbon Sorbents for Oil. *Chem. Chem. Technol.* **2018**, *12*(3), 337–340. <https://doi.org/10.23939/chcht12.03.337>

- [14] Scherrer, P.; Mille, G. Biodegradation of Crude Oil in an Experimentally Polluted Peaty Mangrove Soil. *Mar. Pollut. Bull.* **1989**, *20(9)*, 430–432. [https://doi.org/10.1016/0025-326X\(89\)90061-1](https://doi.org/10.1016/0025-326X(89)90061-1)
- [15] Poyedinok, N.; Belan, M.; Grishchenko, G. Biodestruction of Water-Oil, Run-off Hydrocarbons by Mixed Culture Microorganisms. *Biotechnol. Lett.* **1995**, *17(11)*, 1273–1278. <https://doi.org/10.1007/BF00128401>
- [16] Miller, J.I.; Techtmann, S.; Fortney, J.; Mahmoudi, N.; Joyner, D.; Olesen, S.; Alm, E.; Fernandez, A.; Gardinali, P. et al. Oil Hydrocarbon Degradation by Caspian Sea Microbial Communities. *Front. Microbiol.* [Online] **2019**, *10*, 995. <https://doi.org/10.3389/fmicb.2019.00995>. (accessed Oct 03, 2022).
- [17] Heider, J.; Spormann, A.M.; Beller, H.R.; Widdel, F. Anaerobic Bacterial Metabolism of Hydrocarbons. *FEMS Microbiol. Rev.* **1999**, *22(5)*, 459–473. <https://doi.org/10.1111/j.1574-6976.1998.tb00381.x>
- [18] Labutova, N.M. Sposob Vydeleniya Shtammov Mikroorganizmov-Destruktorov Nefti. RU2624667C1, July 5, 2017.
- [19] Ellis, B.; Balba, M.T.; Theile, P. Bioremediation of Oil Contaminated Land. *Environ. Technol.* **1990**, *11(5)*, 443–454. <https://doi.org/10.1080/09593339009384884>
- [20] Chugunov, V.A.; Ermolenko, Z.M.; Zhigletsova, S.K.; Martovetskaya, I.I.; Mironova, R.I.; Zhirkova, N.A.; Kholodenko, V.P.; Urakov, N.N. Development and Application of a Liquid Preparation with Oil-Oxidizing Bacteria. *Appl. Biochem. Microbiol.* **2000**, *36(6)*, 577–581. <https://doi.org/10.1023/A:1026696506947>
- [21] Chobotarov, A.; Volkogon, M.; Voytenko, L.; Kurdish, I. Accumulation of Phytohormones by Soil Bacteria *Azotobacter vinelandii* and *Bacillus subtilis* under the Influence of Nanomaterials. *J. Microbiol. Biotechnol. Food Sci.* **2017**, *7(3)*, 271–274. <http://doi.org/10.15414/jmbfs.2017/18.7.3.271-274>
- [22] Krupska, T.V.; Turova, A.A.; Gun'ko, V.M.; Turov, V.V. Influence of Highly Dispersed Materials on Physiological Activity of Yeast Cells. *Biopolym. Cell.* **2009**, *25(4)*, 290–297. <http://doi.org/10.7124/bc.0007E8>
- [23] Turov, V.V.; Gun'ko, V.M. *Klasterizovannaya voda i puti ee ispol'zovaniya*; Naukova Dumka: Kyiv, 2011.
- [24] Turov, V.V.; Gun'ko, V.M.; Pakhlov, E.M.; Krupska, T.V.; Tsapko, M.D.; Charmas, B.; Kartel, M.T. Influence of Hydrophobic Nanosilica and Hydrophobic Medium on Water Bound in Hydrophilic Components of Complex Systems. *Colloids Surf. A Physicochem. Eng. Asp.* **2018**, *552*, 39–47. <https://doi.org/10.1016/j.colsurfa.2018.05.017>
- [25] Protsak, I.; Gun'ko, V.M.; Turov, V.V.; Krupska, T.V.; Pakhlov, E.M.; Zhang, D.; Dong, W.; Le, Z. Nanostructured Polymethylsiloxane/Fumed Silica Blends. *Materials* **2019**, *12(15)*, 2409. <https://doi.org/10.3390/ma12152409>
- [26] Krupskaya, T.V.; Gun'ko, V.M.; Protsak, I.S.; Yelahina, N.V.; Turov, V.V. Composites Based on Succinic Acid and Fumed Amorphous Silicas. *Theor. Exp. Chem.* **2020**, *56(1)*, 50–56. <https://doi.org/10.1007/s11237-020-09640-8>
- [27] Gun'ko, V.M.; Turov, V.V. *Nuclear Magnetic Resonance Studies of Interfacial Phenomena*, 1<sup>st</sup> ed.; Taylor & Francis, 2013. <https://doi.org/10.1201/b14202>
- [28] Aksnes, D.W.; Kimtys, L. <sup>1</sup>H and <sup>2</sup>H NMR Studies of Benzene Confined in Porous Solids: Melting Point Depression and Pore Size Distribution. *Solid State Nucl. Magn. Reson.* **2004**, *25(1-3)*, 146–152. <https://doi.org/10.1016/j.ssnmr.2003.03.001>
- [29] Petrov, O.V.; Furo, I. NMR Cryoporometry: Principles, Applications and Potential. *Prog. Nucl. Magn. Reson. Spectrosc.* **2009**, *54(2)*, 97–122. <https://doi.org/10.1016/j.pnmrs.2008.06.001>
- [30] Glushko, V.P. *Termodinamicheskiye svoystva individualnykh veshchestv*; Nauka: Moscow, 1978.

Received: July 30, 2021 / Revised: October 04, 2021 / Accepted: October 22, 2021

#### ГІДРАТНІ ВЛАСТИВОСТІ КОМПЗИТНИХ СИСТЕМ ДЛЯ РЕМЕДІАЦІЇ ВОДИ ТА ҐРУНТІВ НА ОСНОВІ НАНОКРЕМНЕЗЕМУ ТА ДРІЖДЖОВИХ КЛІТИН

**Анотація.** Методом низькотемпературної <sup>1</sup>H ЯМР-спектроскопії досліджено гідратні властивості біонаноккомпозиту, створеного на основі суміші гідрофобного та гідрофільного кремнеземів (АМІ-300 та А-300, у співвідношенні 1:1), води, n-декану і дріжджових клітин. Отримана суміш нанокремнеземів сприяє мітозу та росту клітин. Показано, що причина активації процесів їхньої життєдіяльності може бути пов'язана з утворенням системи водних поліасоціатів, які змінюють умови перенесення речовини через клітинні мембрани, на межі розділу фаз твердих частинок і водного середовища.

**Ключові слова:** <sup>1</sup>H ЯМР-спектроскопія, сильно- та слабоасоційована вода, ремедіація, хлібокарські дріжджі.